

Charged Tags for the Identification of Oxidative Drug Metabolites Based on Electrochemistry and Mass Spectrometry

Alexandra Gutmann,^[a] Lars Julian Wesenberg,^[a] Nadine Peez,^[a, b] Siegfried R. Waldvogel,^{*,[a]} and Thorsten Hoffmann^[a]

In memory of Prof. Dr. Jun-ichi Yoshida


Most of the active pharmaceutical ingredients like Metoprolol are oxidatively metabolized by liver enzymes, such as Cytochrome P450 monooxygenases into oxygenates and therefore hydrophilic products. It is of utmost importance to identify the metabolites and to gain knowledge on their toxic impacts. By using electrochemistry, it is possible to mimic enzymatic transformations and to identify metabolic hot spots. By introducing charged-tags into the intermediate, it is possible to detect and isolate metabolic products. The identification and synthesis of initially oxidized metabolites are important to understand possible toxic activities. The gained knowledge about the metabolism will simplify interpretation and predictions of metabolic pathways. The oxidized products were analyzed with high performance liquid chromatography-mass spectrometry using electrospray ionization (HPLC-ESI-MS) and nuclear magnetic resonance (NMR) spectroscopy. For proof-of-principle, we present a synthesis of one pyridinated main oxidation product of Metoprolol.


Most of the active pharmaceutical ingredients are oxidatively transformed by the liver into metabolites. In order to evaluate pharmacologic or even toxic effects, it is of high importance to know the metabolic products and to gain knowledge about their potential health impacts.^[1,2,3] Biotransformation reactions in the liver mainly lead to hydrolysis or oxidation (phase-1 drug metabolism) and biosynthetic reactions conjugating metabo-

lites with glutathione, sulfates, amino acids or acetates (phase-2 drug metabolism, leads to deactivated metabolites).^[3-5] Phase-1 metabolism is mainly performed (75%) by Cytochrom P450 monooxygenases.^[5,6] It is assumed that Cytochrom P450 monooxygenases use electrophilic oxoferryl-porphyrin-cation radicals to catalyze *N*-dealkylation, *O*-dealkylation, aromatic hydroxylation, oxidation of alcohols and aldehydes and Baeyer-Villiger oxidations.^[2,6-9] Application of electrochemistry in this field is intended to partly simulate the enzymatic oxidation of Cytochrome P450 to form metabolic products of the phase-1 metabolism.^[3,8] Besides the cost-benefit assessment, it is also of great interest for ethical reasons to find alternatives to in vivo experiments.^[5,10] Furthermore, electrochemical synthesis might enable quantitative synthesis of metabolites and reduction of critical waste due to the absence of any reducing and/or oxidizing reagents. Consequently, electrochemistry has already been employed in drug metabolism research.^[7,11] Direct hydroxylation of aromatic compounds leads to labile intermediates that are significantly more prone to further oxidation. Therefore, usually over-oxidized reaction products are formed. Using an electrochemical oxidation system with addition of nucleophilic compounds, which can trap the radical-cationic intermediates, it is possible to detect and isolate these metabolic products. The electrochemical C–H amination of aromatic compounds in the presence of pyridine has already been reported.^[12,13] Pyridine as tag molecule is suitable for the following reasons: the high oxidation potential of pyridine enables selective oxidation of aromatic compounds in the presence of pyridine, furthermore the nucleophilic nature and the excessive use of pyridine lead to a trapping mechanism of occurring radical cation being electrochemically generated. After a second oxidation step the *N*-arylpyridinium cation will be formed. Yoshida and co-workers postulated that any over-oxidation is suppressed because of strong electron-withdrawing effect of a positive charge on the pyridinium nitrogen and the electrostatic repulsion towards the positively polarized anode, avoiding introduction of multiple groups and subsequent degradation.^[12] Therefore, accumulation of the main oxidation product takes place and the most reactive positions in a molecule might reveal metabolic hot spots of a drug entity. When charged tags are incorporated into the target molecules not only the reactive sites of initial oxidation are marked, also the metabolite detection with mass spectrometry is facilitated. Subsequent

[a] A. Gutmann, L. J. Wesenberg, N. Peez, Prof. Dr. S. R. Waldvogel, Prof. Dr. T. Hoffmann
Department of Chemistry
Johannes Gutenberg University Mainz
Duesbergweg 10–14
55128 Mainz (Germany)
E-mail: waldvogel@uni-mainz.de

[b] N. Peez
Institute for Integrated Natural Sciences
University of Koblenz
Universitätsstraße 1
56072 Koblenz (Germany)

 Supporting information for this article is available on the WWW under <https://doi.org/10.1002/open.202000084>

 © 2020 The Authors. Published by Wiley-VCH Verlag GmbH & Co. KGaA. This is an open access article under the terms of the Creative Commons Attribution Non-Commercial License, which permits use, distribution and reproduction in any medium, provided the original work is properly cited and is not used for commercial purposes.

introduction of OH-groups enables synthesis of real drug metabolites.^[14,15]

Metoprolol was chosen as a test molecule for proof-of-principle. Metoprolol is a selective β_1 -receptor blocker and it is mainly used to treat high blood pressure and to prevent further heart problems after myocardial infarction. It is also used when conditions with chest pain occur due to poor blood supply to the heart and abnormally fast heart rate. Metoprolol metabolism has been investigated in many studies over decades.^[16] The electrochemical adaption seems to proceed by the initial one-electron oxidation of an aromatic compound **1** to produce the radical cation. Pyridine is present in abundantly amounts and leads to a subsequent nucleophilic attack on the radical cation species followed by one electron oxidation and elimination of a proton gives the arylpyridinium ion **2** (Scheme 1)

This work presents a reliable and cost-efficient method for synthesizing tagged and oxidized Metoprolol derivatives via electrochemistry and identification with high performance liquid chromatography-mass spectrometry using electrospray ionization (HPLC-ESI-MS) and nuclear magnetic resonance (NMR) spectroscopy. The work is focused on the identification of the main oxidation product and the optimization of the method with respect to yield the major product from oxidation.

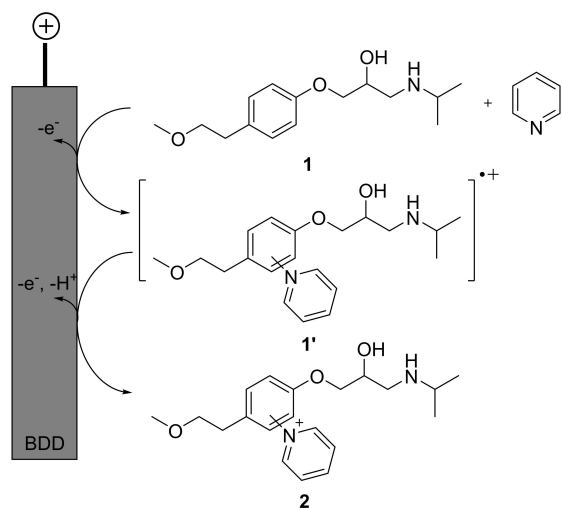
The galvanostatic electrolysis of Metoprolol was carried out in divided cells. Electrosynthesis in presence of pyridine favoured one main oxidation product **2** with a m/z ratio of 345 (positive mode). Structural clarification based on interpretation of MS^2 -, MS^3 - and 2-dimensional nuclear magnetic resonance

(NMR) data revealed following pyridinated charge tag **2** (Figure 1).

Structural isomers containing *N*-pyridinium tags at side chains are suppressed due to inaccessibility of $C(sp^3)$ -H moieties for anodic oxidation.^[17] However, especially at higher applied charge (5 F) beside the main oxidation products other pyridinated side oxidation products (**3**) were detected. Apart from single aromatic pyridination, aliphatic positions were oxidized and transformed into advanced degraded products. Especially, amine and alcohol functionalities are facilitated for these over-oxidation processes (for detailed structure analysis see Supporting Information, chapter 1.4). Beside pyridinium-tagged products, traces of non-pyridinated side oxidation products (**4**) were observed. MS^2 -experiments of these products show similarity with Metoprolol spectra.^[18] Oxidation products of this group contain a modified *O*-containing functional group instead of a pyridinium tag. This suggests that a competitive reaction mechanism occurs during electrolysis. The used boron-doped diamond (BDD)-electrode is thought to enable an 'indirect' electron transfer via OH radicals if water content is significant.^[19] Spectra and postulated structures are provided in the supplementary material (see Supporting Information, chapter 1.4).

Screening of electrochemical reaction conditions were carried out in divided Teflon cells with different separator materials e.g. glass frit or a proton exchange membrane like FAPQ® (for more details see Supporting Information, chapter 1.1). This screening technique is very time efficient and allows the variation of several parameters simultaneously, e.g. current density and applied charge (for more details see Supporting Information chapter 1.1).^[20] Platinum was used as the cathode material due to its low over-potential for the required hydrogen evolution ($\eta^{H_2} = -0.40$ V vs. Ag/AgCl).^[21-23] The BDD electrode was chosen due to the extraordinary properties of BDD as electrode material for electro-organic synthesis.^[24] BDD is well known for its high robustness in electrochemical reactions and large chemical window, caused by high over-potential for the evolution of molecular hydrogen and oxygen ($\eta^{H_2} = -1.10$ V vs. Ag/AgCl; $\eta^{O_2} = 2.30$ V vs. Ag/AgCl).^[21-23] Besides these beneficial electro-organic properties, BDD was already used to mimic enzymatic oxidation reactions.^[25]

The influence of supporting electrolytes such as lithium perchlorate ($LiClO_4$), ammonium acetate (NH_4OAc), and the absence of any supporting electrolyte has been investigated (applied charge 2.5 F, current density: 1 mA/cm², Metoprolol: 0.25 mmol, separation: glass frit). Results were normalized within this test sequence. An insufficient reproducibility was observed, when $LiClO_4$ was used as supporting electrolyte. This could be related to precipitation of the supporting electrolyte. Another disadvantage was the tedious workup procedure, regarding the removal of $LiClO_4$. Ammonium acetate (NH_4OAc) is vaporizable (decomposition at 90 °C). No workup procedure for the crude product after electrolysis is needed for measurements with ESI-MS-systems. Even though 4% water needed to be added to enhance solubility of ammonium acetate and increase conductivity. Applying $LiClO_4$ and NH_4OAc a similar relative conversion to main oxidation products **2** of $71 \pm 3\%$ and $71 \pm 5\%$ could be obtained, respectively. However, without



Scheme 1. Proposed mechanism of anodic oxidation of Metoprolol **1**.

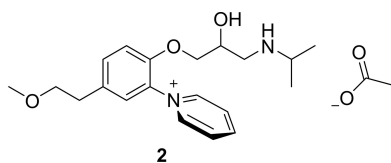


Figure 1. Main oxidation product of Metoprolol in presence of pyridine. For more information on the analytical data see Supporting Information.

supporting electrolytes the relative result of 65 ± 2 % main oxidation product is decreased. To ensure conductivity a water content of 4.5 % was applied in the anodic half-cell. Increased water contents in anodic half-cells led to an enhanced formation of OH radicals and therefore increased formation of non-pyridinated side oxidation products (4) (see table 1)

Subsequently, we investigated the efficiency of Metoprolol electrooxidation. Experimental data indicates that the conversion depends on the Metoprolol concentration containing 20.8 mmol/L (0.125 mmol Metoprolol), 41.7 mmol/L (0.250 mmol Metoprolol) and 62.5 mmol/L (0.375 mmol Metoprolol) (supporting electrolyte: NH_4OAc , current density: 1 mA/cm² with 2.5 F applied charge, separation: glass frit). Results were normalized within this test sequence. With decreased Metoprolol concentration (0.125 mmol) lowest Metoprolol conversion has been observed (see table 2). Best results of the formation of compound 2 were obtained with 0.250 mmol Metoprolol, while increased Metoprolol concentration (0.375 mmol Metoprolol) decreased relative yields of 2 from 87 % to 67 % respectively. Further increased formation of non-pyridinium-tagged oxidation products (4) was obtained. A Metoprolol concentration of 41.67 mmol/L (0.250 mmol) seems to be optimal for the formation of 2.

Next, the influence of the separator material was investigated. Due to their positive charge, pyridinium-tagged derivatives are prevented from further oxidation from the anode. However, oxidized positive charged intermediates or products are attracted by the cathode. Furthermore, the concentration gradient between anodic and cathodic compartments increases during electrolysis. Both effects lead to an

increasing trend of oxidation products diffusing towards the cathode. For preventing migration of oxidation products and starting material towards the cathodic compartment a divided cell set-up was used with separator membranes. Applied separation membranes require permeaselectivity towards exclusively protons while maintaining low electrical resistivity and prevent diffusion of analytes in the cathodic compartment. Here, porous glass frits and FAPQ® membranes have been compared for their permeaselectivity. Therefore, the analyte concentrations were determined in both half-cells after electrolysis. The values shown in figure 2 were calculated as fraction in the cathodic half-cell to the total sum found in both compartments. Experiments with glass frits as separator membrane have shown that (independently from supporting electrolytes used) 71.2 % of Metoprolol in particular was found in the cathodic compartment (impedes a full conversion, see figure 2A). The backwards diffusion of Metoprolol from the cathodic half-cell to the anodic half-cell seems to be too slow to equilibrate Metoprolol conversion by oxidation. Separation with glass frit also resulted in 20 % of main oxidation product 2 in the cathodic half cell (decreasing obtained yields). An applied FAPQ®-membrane was able to prevent diffusion in the cathodic compartment almost quantitatively for compound 2 and decreased the diffusion of Metoprolol to 4.5 %.

FAPQ® is a proton permeable exchange membrane, (for further details see chapter 1.1). The current density is related to the radical spin density close to the electrode surface. Controlled radical formation is desired, hence lower current densities might be beneficial. Higher current densities tend to lead to uncontrolled reaction pathways, which is certainly undesired with fragile substrates. The influence of the current density on oxidation products formation was investigated for 1 and 10 mA/cm² (supporting electrolyte: NH_4OAc or none, amount of charge: 2.5 F, Metoprolol: 0.25 mmol, separator: glass frit). Increased current density caused a decreased conversion of Metoprolol and the formation

Table 1. Relative conversion dependent on supporting electrolyte and water content (note: Relative yields are based on the highest result in the experiment series (in this case the sum of compounds (3) with LiClO_4 as supporting electrolyte)).

| Supporting electrolyte | Water content | [U_{iv}]=V | 2 ^[a] | 3 ^[b] | 4 ^[c] |
|-------------------------|---------------|----------------|------------------|------------------|------------------|
| LiClO_4 * | 0.0 % | 2.5 | $77 \pm 3\%$ | $100 \pm 2\%$ | $1 \pm 0\%$ |
| NH_4OAc | 4.0 % | 2.9 | $76 \pm 5\%$ | $99 \pm 1\%$ | $4 \pm 1\%$ |
| None | 4.5 % | 3.6 | $70 \pm 2\%$ | $93 \pm 2\%$ | $6 \pm 1\%$ |

*not further pursued, due to lack of reproducibility, [a] 2 = main oxidation product, [b] 3 = pyridinated side oxidation products, [c] 4 = non-pyridinated side oxidation products; U_{iv} = terminal voltage; for electrolysis conditions see text.

Table 2. Influence of provided Metoprolol on product formation (note: Relative yields are based on the highest result in the experiment series (in this case the sum of compounds (3) with 0.250 mmol as supporting electrolyte)).

| Metoprolol molarity | Metoprolol recovery | [U_{iv}]=V | 2 ^[a] | 3 ^[b] | 4 ^[c] |
|---------------------|---------------------|----------------|------------------|------------------|------------------|
| 0.125 mmol | 53 % | 2.4 | 45 % | 56 % | 2 % |
| 0.250 mmol | 6 % | 2.4 | 87 % | 100 % | 5 % |
| 0.375 mmol | 8 % | 2.5 | 67 % | 80 % | 10 % |

[a] 2 = main oxidation product, [b] 3 = pyridinated side oxidation products, [c] 4 = non-pyridinated side oxidation products; U_{iv} = terminal voltage; for electrolysis conditions see text.

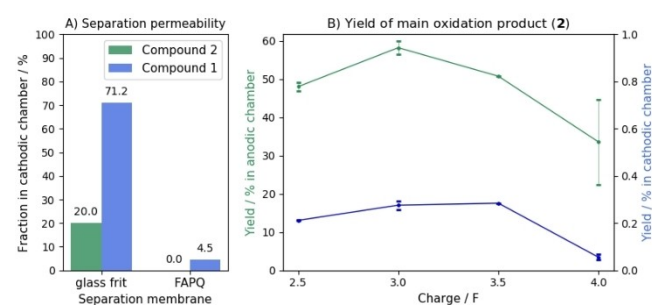


Figure 2. (A): Efficiency of half-cell separation using different membranes. Values were calculated as fraction in cathodic compartment to the total sum found in both half-cells. Separation with glass frit resulted in 20 % of 2 (green) or even above 70 % for Metoprolol (blue). An applied FAPQ membrane was able to prevent diffusion in cathodic compartment almost quantitatively for main oxidation product 2 and decreased diffusion to 4.5 % for Metoprolol. (B): Obtained yield of 2 dependent on applied charge. A maximal formation of compound 2 of $58 \pm 2\%$ was obtained at 3.0 F. The observation of cathodic half-cell concentrations for main oxidation product 2 confirmed that diffusion into the cathodic compartment does not increase with increased applied charge (also resulting in increased reaction time). For error calculation every charge has been applied twice.

of the main oxidation product decreased by 20% (with NH_4OAc as supporting electrolyte) or even 50% (without any supporting electrolyte) respectively. The theoretical amount of charge of Metoprolol is 2 F. The increase of applied charge from 2.5 F stepwise to 5.0 F resulted in depletion of Metoprolol with 3.5 F (see Figure 3, red values). However, increased Metoprolol conversion does not lead to increased formation of the main oxidation product (2, green values). Increased applied charges form pyridinated side oxidation products (3, dark blue) might result from further oxidation of 2. Non-pyridinated side oxidation products (4, light blue) seem not to be heavily affected by increased applied charges (Electrolysis conditions: Charge: 2.5–5 F, stepwise, supporting electrolyte: NH_4OAc , current density: 1 mA/cm^2 , 0.25 mmol Metoprolol, membrane: FAPQ®).

This study enabled synthesis of pyridinium-tagged Metoprolol derivatives and revealed an active side at the *ortho*-position of the phenoxy ether of Metoprolol, while avoiding multi oxidation reactions (one main oxidation product). A maximal formation of main oxidation product 2 via electrolysis of $58 \pm 2\%$ was obtained with supporting electrolyte NH_4OAc , 0.25 mmol Metoprolol content, half-cell separation with FAPQ®-membrane, applied current density of 1 mA/cm^2 and applied charge of 3.0 F. Traces of pyridinium tagged (3) and non-

pyridinium tagged side oxidation products (4) have been minimized. Therefore, oxidized products bearing a pyridinium moiety can be enriched during electrolysis and isolated for metabolite synthesis. Transition metal catalysis of pyridinium substituted groups on specifically selected oxygen nucleophiles might lead to an effective synthesis of metabolic products (Scheme 2). Recently, studies on this field are emerging, focusing on pyridinium salts as redox-active functional group transfer reagents.^[14] Hence, this method might be able to provide a new reliable pathway for the synthesis of metabolites and supports further research into drug metabolism since direct hydroxylation reactions would lead to an over-oxidation caused by lower oxidation potential of the new electron-rich aromatic system. Consequently, further reactions occur, and the original metabolites would be only found in low yields.

Acknowledgements

Support of the Advanced Lab of Electrochemistry and Electrosynthesis – ELYSION (Carl Zeiss Stiftung) is gratefully acknowledged.

Conflict of Interest

The authors declare no conflict of interest.

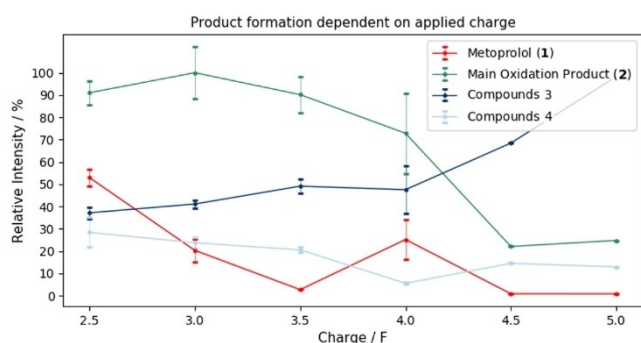
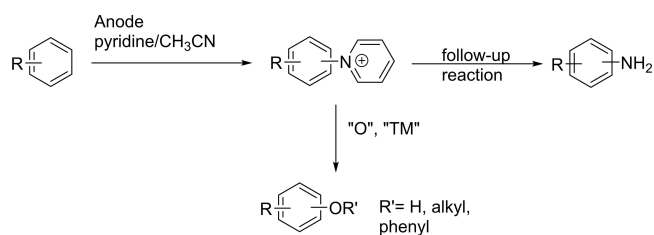


Figure 3. Metoprolol conversion and formation of side products dependent on applied charge. Red data reveal increased conversion of Metoprolol with elevated amount of charge. Increased Metoprolol conversion does not lead to increased formation of the main oxidation product (2, green values). Non-pyridinated side oxidation products (4, light blue) seem to decrease slightly by elevated amount of charges. Increased applied charges form pyridine tagged side oxidation products (3, dark blue) which might result from further oxidation of 2 or derivatization of (4) with pyridine. For error calculation every charge has been applied three times, except 4.5 and 5.0 F, which have been tested only once. For further experimental descriptions see text.



Scheme 2. Anodic oxidation of arenes in presence of pyridine and conversion to metabolites; TM = transition metal

Keywords: anodic oxidation · charged tags · drug metabolites · electrochemistry · mass spectrometry

- [1] a) J. Genovino, D. Sames, L. G. Hamann, B. B. Touré, *Angew. Chem. Int. Ed.* **2016**, *55*, 14218–14238; *Angew. Chem.* **2016**, *128*, 14430–1445; b) S. D. Krämer, B. Testa, *Chem. Biodiversity* **2009**, *6*, 1477–660; c) A. F. Stepan, D. P. Walker, J. Bauman, D. A. Price, T. A. Baillie, A. S. Kalgutkar, M. D. Aleo, *Chem. Res. Toxicol.* **2011**, *24*, 1345–1410; d) B. Testa, S. D. Krämer, *Chem. Biodiversity* **2006**, *3*, 1053–1101.
- [2] J. Johansson, L. Weidolf, U. Jurva, *Rapid Commun. Mass Spectrom.* **2007**, *21*, 2323–2331.
- [3] K. G. Madsen, J. Olsen, C. Skonberg, S. H. Hansen, U. Jurva, *Chem. Res. Toxicol.* **2007**, *20*, 821–831.
- [4] S. Sozzani, D. Bosisio, A. Mantovani, P. Ghezzi, *Eur. J. Immunol.* **2005**, *35*, 3095–3098.
- [5] K. Schroer, M. Kittelmann, S. Lütz, *Biotechnol. Bioeng.* **2010**, *106*, 699–706.
- [6] R. Bernhardt, *J. Biotechnol.* **2006**, *124*, 128–145.
- [7] U. Jurva, H. V. Wikstrom, L. Weidolf, A. P. Bruins, *Rapid Commun. Mass Spectrom.* **2003**, *17*, 800–810.
- [8] F. P. Guengerich, *AAPS J.* **2006**, *8*, E101–11.
- [9] A. Chefson, K. Auclair, *Mol. Biosyst.* **2006**, *2*, 462–469.
- [10] a) H. U. Schulze, H. Staudinger, *Die Naturwissenschaften* **1975**, *62*, 331–340; b) H. Zhang, D. Zhang, W. Li, M. Yao, C. D'Arienzo, Y.-X. Li, W. R. Ewing, Z. Gu, Y. Zhu, N. Murugesan, W.-C. Shyu, W. G. Humphreys, *Drug Metab. Dispos.* **2007**, *35*, 795–805; c) J. Kiebish, W. Holla, J. Heidrich, M. Poraj-Kobielska, M. Sandvoss, R. Simonis, G. Gröbe, J. Atzrodt, M. Hofrichter, K. Scheibner, *Bioorg. Med. Chem.* **2015**, *23*, 4324–4332.
- [11] a) M. K. Eberle, A.-M. Jutzi-Eme, F. Nüniger, *Bioorg. Med. Chem. Lett.* **1995**, *5*, 1725–1728; b) L. R. Hall, R. T. Iwamoto, R. P. Hanzlik, *Am. J. Org. Chem.* **1989**, *54*, 2446–2451; c) S. Khera, N. Hu, *Anal. Bioanal. Chem.* **2013**, *405*, 6009–6018; d) W. Lohmann, R. Dötzer, G. Gütter, S. M. van Leeuwen, U. Karst, *J. Am. Soc. Mass Spectrom.* **2009**, *20*, 138–145; e) R. Stalder, G. P. Roth, *ACS Med. Chem. Lett.* **2013**, *4*, 1119–1123; f) K. Pelivan, L. Frensemeier, U. Karst, G. Koellensperger, B. Bielec, S. Hager, P. Heffeter, B. K. Keppler, C. R. Kowol, *Analyst* **2017**, *142*, 3165–3176; g) T. Wigger, A. Seidel, U. Karst, *Chemosphere* **2017**, *176*, 202–211; h) A. Paci,

- T. Martens, J. Royer, *Bioorg. Med. Chem. Lett.* **2001**, *11*, 1347–1349; i) K. G. Madsen, G. Grönberg, C. Skonberg, U. Jurva, S. H. Hansen, J. Olsen, *Chem. Res. Toxicol.* **2008**, *21*, 2035–2041; j) M. K. Bal, C. E. Banks, A. M. Jones, *ChemElectroChem*. **2019**, *6*, 4284–4291; k) M. H. Rahman, M. K. Bal, A. M. Jones, *ChemElectroChem*. **2019**, *6*, 4093–4104.
- [12] T. Morofuji, A. Shimizu, J.-i. Yoshida, *J. Am. Chem. Soc.* **2013**, *135*, 5000–5003.
- [13] a) S. R. Waldvogel, S. Möhle, *Angew. Chem. Int. Ed.* **2015**, *54*, 6398–6399; *Angew. Chem.* **2015**, *127*, 6496–6497; b) L. J. Wesenberg, S. Herold, A. Shimizu, J. -i Yoshida, S. R. Waldvogel, *Chem. Eur. J.* **2017**, *23*, 12096–12099.
- [14] A. Togni, S. L. Rössler, B. J. Jelier, E. Magnier, G. Dagousset, E. M. Carreira, *Angew. Chem. Int. Ed.* **2019**; *Angew. Chem.* **2019**; in press. [Doi.org/10.1002/anie.201911660].
- [15] D. Moser, Y. Duan, F. Wang, Y. Ma, M. J. O'Neill, J. Cornella, *Angew. Chem. Int. Ed.* **2018**, *57*, 11035–11039; *Angew. Chem.* **2018**, *130*, 11201–11205.
- [16] a) J. C. McGourty, J. H. Silas, M. S. Lennard, G. T. Tucker, H. F. Woods, *Br. J. Clin. Pharmacol.* **1985**, *20*, 555–566; b) S. S. Murthy, H. U. Shetty, W. L. Nelson, P. R. Jackson, M. S. Lennard, *Biochem. Pharmacol.* **1990**, *40*, 1637–1644; c) N. Bodor, P. Buchwald, *AAPS J.* **2005**, *7*, E820–33; d) V. K. H. Barclay, N. L. Tyrefors, I. M. Johansson, C. E. Pettersson, *J. Chromatogr. A* **2012**, *1269*, 208–217; e) T. Xu, S. Bao, P. Geng, J. Luo, L. Yu, P. Pan, Y. Chen, G. Hu, *J. Chromatogr. B* **2013**, *937*, 60–66.
- [17] Q.-L. Yang, Y.-Q. Li, C. Ma, P. Fang, X.-J. Zhang, T.-S. Mei, *J. Am. Chem. Soc.* **2017**, *139*, 3293–3298.
- [18] M. D. Hernando, M. J. Gómez, A. Agüera, A. R. Fernández-Alba, *TrAC Trends Anal. Chem.* **2007**, *26*, 581–594.
- [19] a) M. Panizza, P. A. Michaud, G. Cerisola, C. Comninellis, *J. Electroanal. Chem.* **2001**, *507*, 206–214; b) A. Kirste, G. Schnakenburg, F. Stecker, A. Fischer, S. R. Waldvogel, *Angew. Chem. Int. Ed.* **2010**, *49*, 971–975; *Angew. Chem.* **2010**, *122*, 983–987; c) B. Marselli, J. Garcia-Gomez, P.-A. Michaud, M. A. Rodrigo, C. Comninellis, *J. Electroanal. Chem. Interfacial Electrochem.* **2003**, *150*, D79; d) A. Stefanova, S. Ayata, A. Erem, S. Ernst, H. Baltruschat, *Electrochim. Acta* **2013**, *110*, 560–569.
- [20] C. Gütz, B. Klöckner, S. R. Waldvogel, *Org. Process Res. Dev.* **2016**, *20*, 26–32.
- [21] S. R. Waldvogel, S. Mentizi, A. Kirste, *Top. Curr. Chem.* **2012**, *320*, 1–31.
- [22] S. R. Waldvogel, B. Elsler, *Electrochim. Acta* **2012**, *82*, 434–443.
- [23] S. Lips, S. R. Waldvogel, *ChemElectroChem*. **2019**, *6*, 1649–1660.
- [24] a) J. L. Röckl, D. Pollok, R. Franke, S. R. Waldvogel, *Acc. Chem. Res.* **2020**, *53*, 45–61; b) S. Möhle, M. Zirbes, E. Rodrigo, T. Gieshoff, A. Wiebe, S. R. Waldvogel, *Angew. Chem. Int. Ed.* **2018**, *57*, 6018–6041; *Angew. Chem.* **2018**, *130*, 6124–6149; c) B. Gleede, T. Yamamoto, K. Nakahara, A. Botz, T. Graßl, R. Neuber, T. Matthée, Y. Einaga, W. Schuhmann, S. R. Waldvogel, *ChemElectroChem*. **2019**, *6*, 2771–2776; d) A. Wiebe, T. Gieshoff, S. Möhle, E. Rodrigo, M. Zirbes, S. R. Waldvogel, *Angew. Chem. Int. Ed.* **2018**, *57*, 5594–5619; *Angew. Chem.* **2018**, *130*, 5694–5721.
- [25] a) H. Faber, D. Melles, C. Brauckmann, C. A. Wehe, K. Wentker, U. Karst, *Anal. Bioanal. Chem.* **2012**, *403*, 345–354; b) P. Mielczarek, M. Smoluch, J. H. Kotlinska, K. Labuz, T. Gotszalk, M. Babij, P. Suder, J. Silberring, *J. Chromatogr. A* **2015**, *1389*, 96–103.

Manuscript received: March 27, 2020